

# Base-Free Direct Oxidation of 1-Octanol to Octanoic Acid and its Octyl Ester over Supported Gold Catalysts

Tamao Ishida,<sup>\*,[a, f]</sup> Yuichiro Ogihara,<sup>[b]</sup> Hironori Ohashi,<sup>[c, f]</sup> Tomoki Akita,<sup>[d, f]</sup> Tetsuo Honma,<sup>[e]</sup> Hiroshi Oji,<sup>[e]</sup> and Masatake Haruta<sup>\*,[b, f]</sup>

The choice of a suitable support for gold nanoparticles (Au NPs) enabled the direct oxidation of unreactive aliphatic alcohol, 1-octanol, to octanoic acid and octyl octanoate in the absence of a base. Under optimized conditions, Au NPs supported on NiO (Au/NiO) exhibited remarkably high catalytic ac-

tivities and excellent selectivities to octanoic acid (e.g., 97%) at full conversion. In contrast to Au/NiO, Au/CeO<sub>2</sub> selectively produced octyl octanoate as a major product in a base-free aqueous solution with a maximum selectivity of 82% under optimized conditions.

## Introduction

The oxidation of alcohols into aldehydes and carboxylic acids is one of the most fundamental and important transformations in the chemical industry. From the point of view of green chemistry, replacing stoichiometric oxidants with heterogeneous catalytic systems combined with clean and inexpensive molecular oxygen is very desirable.<sup>[1]</sup> Until now, many types of heterogeneous catalysts based on Ru, Pd, Pt, and Au have been reported for aerobic oxidation of alcohols.<sup>[2]</sup> These processes usually yield aldehydes in the absence of a base, whereas further oxidation to carboxylic acids or esters requires basic conditions even over active Pd- and Pt-based catalysts.<sup>[3]</sup> When alcohol oxidations are conducted under basic conditions, carboxylates must be neutralized with inorganic acids, generating large amounts of waste inorganic salts. Thus, the base-free direct oxidation of alcohols to carboxylic acids and esters is an ideal green process. Although several catalytic systems have been reported to promote the production of carboxylic acids under base-free conditions,<sup>[4]</sup> only one report exists on the oxidation of less reactive aliphatic alcohols to carboxylic acids, describing high selectivity over unsupported platinum nanoparticles (Pt NPs).<sup>[5]</sup>

Supported Au NPs have attracted a growing interest for the aerobic oxidation of alcohols owing to their high product selectivity without the need for doping hazardous metals such as Pb or Bi.<sup>[6]</sup> In principle, metal-oxide-supported Au catalysts as well as other noble-metal catalysts require the addition of a base to achieve carboxylic acids or esters from alcohols. Base-free oxidation of alcohols to carboxylic acids was successfully achieved only upon the addition of oxidants such as hydrogen peroxide.<sup>[7]</sup>

Christensen and co-workers first reported the direct aerobic oxidation of ethanol to acetic acid in water under base-free conditions over Au/MgAl<sub>2</sub>O<sub>4</sub>.<sup>[8]</sup> We reported that Au NPs supported on simple metal oxides such as NiO promoted the base-free oxidation of methanol<sup>[9a]</sup> and ethanol.<sup>[9b]</sup> Prati and co-workers studied the base-free oxidation of 1-octanol with O<sub>2</sub> over Au NPs supported on nanometer-sized NiO.<sup>[10]</sup> These au-

thors reported the formation of octanoic acid, although at moderate conversion and with low selectivity (31%).

In this work, we selected 1-octanol as a model substrate to study the oxidation of aliphatic alcohols to carboxylic acids and alkyl esters with high selectivity in the absence of a base. Au NPs supported on various types of metal oxides were screened, with Au/NiO exhibiting remarkably high catalytic activity and selectivity to octanoic acid. The size and chemical state of Au on NiO were characterized by transmission electron microscopy (TEM) observations and X-ray absorption fine structure (XAFS) measurements, revealing the presence of small Au NPs deposited on NiO. Unlike Au/NiO, Au/CeO<sub>2</sub> was found to be a selective catalyst for the production of octyl octanoate.

[a] Dr. T. Ishida

Department of Chemistry, Faculty of Sciences  
Kyushu University  
6-10-1 Hakozaki, Higashi-ku, Fukuoka 812-8581 (Japan)  
Fax: (+81) 92-642-7528  
E-mail: tishida@chem.kyushu-univ.jp

[b] Y. Ogihara, Prof. Dr. M. Haruta

Department of Applied Chemistry  
Graduate School of Urban Environmental Sciences  
Tokyo Metropolitan University  
1-1 Minami-osawa, Hachioji, Tokyo 192-0397 (Japan)  
Fax: (+81) 42-677-2851  
E-mail: haruta-masatake@center.tmu.ac.jp

[c] Dr. H. Ohashi

Faculty of Arts and Science  
Kyushu University  
744 Motoooka, Nishi-ku, Fukuoka 819-0395 (Japan)

[d] Dr. T. Akita

Research Institute for Ubiquitous Energy Devices  
National Institute of Advanced Industrial Science and Technology  
1-8-31 Midorigaoka, Ikeda, Osaka 563-8577 (Japan)

[e] Dr. T. Honma, Dr. H. Oji

Japan Synchrotron Radiation Research Institute (JASRI)/Spring-8  
1-1-1 Kouto, Sayo, Hyogo 679-5198 (Japan)

[f] Dr. T. Ishida, Dr. H. Ohashi, Dr. T. Akita, Prof. Dr. M. Haruta

Japan Science and Technology Agency (JST), CREST  
4-1-8 Hon-cho, Kawaguchi, Saitama 332-0012 (Japan)

## Results and Discussion

## Characterization of Au/NiO

Au on NiO was prepared by a conventional co-precipitation (CP) method.<sup>[11]</sup> Figure 1 shows a high-angle annular dark-field

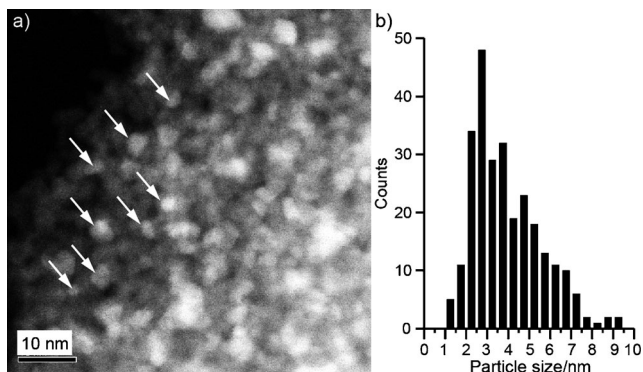


**Figure 1.** a) HAADF-STEM image of Au/NiO, and b) size distribution of Au NPs. The white arrows indicate Au NPs.

scanning TEM (HAADF-STEM) image as well as the size distributions of Au NPs supported on NiO. The mean diameter of the Au NPs was calculated to be  $4.0 \pm 2.0$  nm, while the size of NiO particles ranged from 3 to 5 nm in a material with a specific surface area of  $203 \text{ m}^2 \text{ g}^{-1}$ . With the aim to elucidate the chemical state and the size of Au NPs supported on NiO, XAFS measurements were performed. Figure 2 shows the Au  $L_3$ -edge

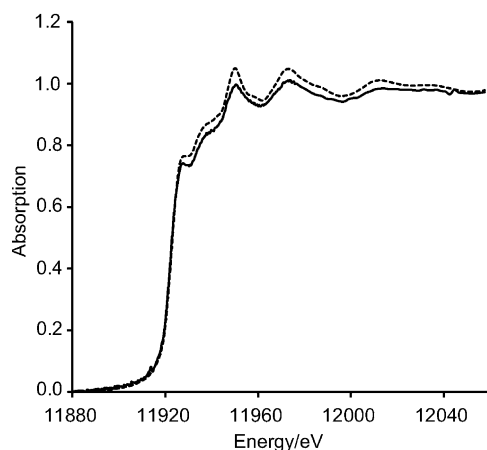


**Figure 2.** Au  $L_3$ -edge XANES spectra of Au/NiO (solid line) and Au foil (dashed line).

XANES spectra of Au/NiO. A white line was not observed for Au/NiO, thereby indicating that the chemical state of Au NPs on NiO was  $\text{Au}^0$ . Figures 3–4 and Table 1 show the  $k^3$ -weighted EXAFS spectra, radial structure functions, and EXAFS fit parameters, respectively. The amplitude of the EXAFS oscillation (Figure 3) and the magnitude of the radial structure functions of Au/NiO (Figure 4) were lower than those of Au foil. This can

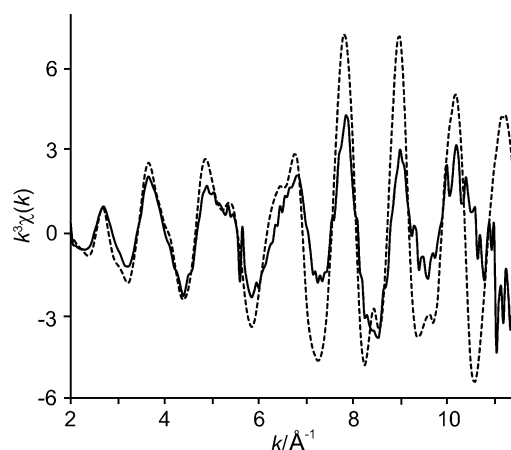


**Figure 3.**  $k^3$ -weighted Au  $L_3$ -edge EXAFS oscillations of Au/NiO (solid line) and Au foil (dashed line).

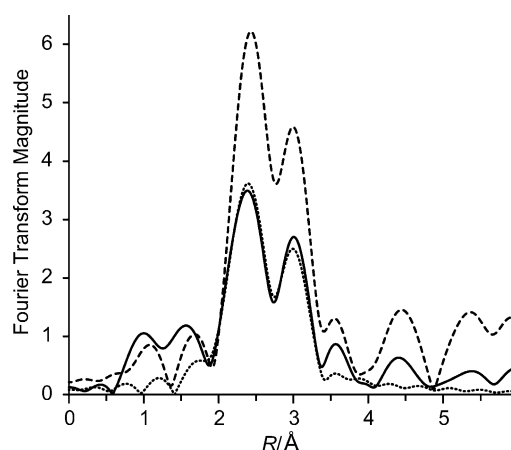


**Figure 4.** Radial structure functions of Au/NiO (solid line) and Au foil (dashed line). Dotted line indicates the fitted line for Au/NiO.

**Table 1.** EXAFS fit parameters for Au/NiO ( $k^3$ :  $\Delta k = 2\text{--}10 \text{ \AA}^{-1}$  and  $\Delta r = 1.9\text{--}3.4 \text{ \AA}$ ). Intrinsic loss factor,  $S_0^2 = 0.894$  (Au–Au from Au foil data)

Sample	Shells	CN <sup>[a]</sup>	$R$ [ $\text{\AA}$ ] <sup>[b]</sup>	$\sigma^2$ [ $\text{\AA}^2$ ] <sup>[c]</sup>	$R_{\text{factor}}$ [%] <sup>[d]</sup>
Au foil	Au–Au	12.0 <sup>[e]</sup>	$2.863 \pm 0.003$	$0.0080 \pm 0.0005$	–
Au/NiO	Au–Au	$10.0 \pm 0.9$	$2.85 \pm 0.01$	$0.011 \pm 0.001$	0.023

[a] First shell coordination number. [b] Bond length. [c] Debye–Waller factor. [d] Goodness-of-fit index. [e] Coordination number was fixed as that of a fcc lattice.

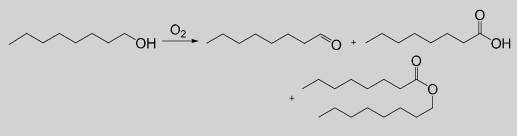
be partly produced by an increase in the Debye–Waller factor of Au/NiO, which accounts for the disorder in the crystal structure of Au NPs. Another factor responsible for the lower magnitude of EXAFS oscillation and radial structure functions is the decrease in the coordination number (CN) of Au atoms. The curve-fitting analysis revealed an average CN for Au/NiO of  $10.0 \pm 0.9$ , which was lower than that found in Au foil (12.0). This CN value in Au/NiO corresponded to a Au NPs diameter of about 2.5 nm.<sup>[12]</sup> These results indicate that Au NPs were mainly dispersed on NiO in a size ranging from 2–4 nm. The

average size of Au NPs calculated from XAFS measurements was smaller than that estimated by HAADF-STEM. This might be ascribed to the difficulty in finding small Au NPs located inside the support and/or dispersed on aggregated nanometer-sized NiO particles by TEM.

### Oxidation of 1-octanol to octanoic acid

Gold NPs supported on a variety of metal oxides were screened for the base-free aerobic oxidation of 1-octanol in water (Table 2). Gold NPs supported on basic metal oxides

**Table 2.** Aerobic oxidation of 1-octanol over Au, Pd, and Pt nanoparticles supported on metal oxides in water.<sup>[a]</sup>



Entry	Catalyst	Conv. <sup>[b]</sup> [%]	Selectivity [%] <sup>[b]</sup>		
			octanal	octanoic acid	octyl octanoate
1	Au/Al <sub>2</sub> O <sub>3</sub>	54	2	26	63
2	Au/TiO <sub>2</sub>	34	3	41	56
3	Au/MnO <sub>2</sub>	33	6	12	30
4	Au/Fe <sub>2</sub> O <sub>3</sub>	57	4	14	26
5	Au/Co <sub>3</sub> O <sub>4</sub>	12	33	< 1	< 1
6	Au/NiO	90	0	68	28
7	Au/ZnO	30	7	7	57
8	Au/ZrO <sub>2</sub>	52	2	30	68
9	Au/CeO <sub>2</sub>	23	9	0	91
10	Pd/NiO	4	50	0	0
11	Pt/NiO	0	0	0	0

[a] Reaction conditions: 1-octanol (8 mmol), H<sub>2</sub>O (3 mL), catalyst (metal 0.1 mol%), O<sub>2</sub> (0.5 MPa), 100 °C, 18 h. [b] Calculated on the basis of GC analysis using anisole as an internal standard.

showed catalytic activities superior to neutral or acidic oxides, as basic oxides facilitate deprotonation of hydroxy groups. However, the activity order did not directly correlate to the basicity of the supports. In addition, octyl octanoate was obtained as a major product together with octanoic acid. These results contrast with previous reports in which Au catalysts yielded aldehydes as a major product in the absence of a base.<sup>[5]</sup> The utilization of a higher concentration of a substrate would lead to a further oxidation of octanal with 1-octanol forming octyl octanoate. The same tendency was reported by Prati and co-workers, as observed under high concentrations of substrates in cyclohexane.<sup>[10]</sup> The only exception was Au/Co<sub>3</sub>O<sub>4</sub>, which mainly produced octanal (entry 5). Gold on CeO<sub>2</sub> showed the highest selectivity to octyl octanoate at relatively low conversion (entry 9). Among the different materials tested, Au/NiO exhibited the highest catalytic activity and selectivity to octanoic acid (entry 6). Palladium on NiO (entry 10) and Pt/NiO (entry 11), although being prepared in a similar manner to Au/NiO (e.g., CP), showed poor catalytic activities.

Reaction conditions were optimized to improve the selectivity to octanoic acid over Au/NiO (Table 3). Gold on NiO was

**Table 3.** Optimization of reaction conditions for the production of octanoic acid over Au/NiO.<sup>[a]</sup>

Entry	Solvent	Conv. <sup>[b]</sup> [%]	Selectivity [%] <sup>[b]</sup>		
			octanal	octanoic acid	octyl octanoate
1	toluene	29	34	0	59
2	1,4-dioxane	5	60	0	0
3	MeCN	5	0	0	0
4	solvent-free	44	9	36	36
5	H <sub>2</sub> O (12 mL)	83	0	66	20
6 <sup>[e]</sup>	H <sub>2</sub> O/dioxane <sup>[c]</sup>	22	23	55	5
7	H <sub>2</sub> O/MeCN <sup>[d]</sup>	19	16	37	42
8	H <sub>2</sub> O/toluene <sup>[d]</sup>	31	29	74	26
9 <sup>[e,f]</sup>	H <sub>2</sub> O/dioxane <sup>[c]</sup>	41	20	51	5
10 <sup>[g,h]</sup>	H <sub>2</sub> O/dioxane <sup>[c]</sup>	70	4	91	4
11 <sup>[g,i]</sup>	H <sub>2</sub> O/dioxane <sup>[c]</sup>	95	0	98	2
12 <sup>[g,j]</sup>	H <sub>2</sub> O/dioxane <sup>[c]</sup>	> 99	0	97	2
13 <sup>[g,k]</sup>	H <sub>2</sub> O/dioxane <sup>[c]</sup>	76	1	66	15

[a] Reaction conditions: 1-octanol (8 mmol), solvent (3 mL), Au/NiO (Au 0.1 mol%), O<sub>2</sub> (0.5 MPa), 100 °C, 18 h. [b] Calculated on the basis of GC analysis using anisole as an internal standard. [c] 1:3 v/v ratio. [d] 1:1 v/v ratio. [e] 1-Octanol (2.7 mmol). [f] Au 0.3 mol%. [g] 1-octanol (2.7 mmol), solvent (12 mL). [h] Au 1 mol%. [i] Au 3 mol%. [j] Au 3 mol%, 48 h. [k] Au/CeO<sub>2</sub> (Au 3 mol%).

almost inactive in 1,4-dioxane and acetonitrile and only small amounts of octanal were obtained in 1,4-dioxane (entry 2). In contrast, Au/NiO was relatively active in toluene as compared to dioxane, and octyl octanoate was obtained as a major product (entry 1). This was due to the further oxidation of octanal with 1-octanol. Under solvent-free conditions, the reaction proceeded unselectively and both octanoic acid and octyl ester were produced in roughly similar amounts (entry 4). Water proved to be a good solvent for producing octanoic acid (Table 2, entry 6), even though 1-octanol is immiscible in water. A mixture of 1,4-dioxane and H<sub>2</sub>O was reported to be an efficient solvent for the oxidation of benzyl alcohol to benzoic acid over Pt/C.<sup>[4]</sup> As the formation of octyl octanoate is assumed to be favored by high concentrations of 1-octanol, organic solvents were added to water to make 1-octanol miscible in the reaction solution. With the aim to generate a single-phase reaction solution, a 1:3 v/v water/organic solvent ratio was used (a lower ratio in the case of the water/1,4-dioxane mixture) and the concentration of the substrate was decreased. Even though the reaction rate was decreased, the ester selectivity was reduced in the water/1,4-dioxane mixture (Table 3, entry 6) compared with other reaction media (entries 7 and 8). Since the reaction did not proceed in pure 1,4-dioxane (entry 2), peroxides (formed by decomposition of 1,4-dioxane) are unlikely to play a key role in the octanol oxidation in water/1,4-dioxane. An increase in the amount of Au/NiO (Au 0.3 mol%) improved the conversion while maintaining the product selectivity (entry 9). A further increase in the amount of Au (1 mol%) combined with a decrease in the substrate concentration led to a noticeable increase in the selectivity to octanoic acid (entry 10). Lower concentrations of the substrate slightly suppressed the formation of octyl octanoate (entry 5). Thus, the observed high selectivity was mainly ascribed to an increase in the amount of Au. Upon increasing the amount of

Au/NiO, octanal would be more prone to react with water adsorbed on Au/NiO surfaces. This would lead to high selectivities to octanoic acid. Consequently, an excellent selectivity (98%) was achieved under optimized conditions (entry 11) and this selectivity was maintained at full conversion after 48 h (entry 12). The reaction was also performed in the presence of Au/CeO<sub>2</sub> under optimized conditions (entry 13). Although the selectivity to octanoic acid was greatly improved, octyl octanoate was also obtained in significant amounts (15%). The differences in the product distributions over the Au/NiO catalyst prepared by Prati<sup>[10]</sup> and that prepared herein are mainly ascribed to the different reaction media employed, although the metal oxide surface properties also affect the selectivity.

### Oxidation of 1-octanol to octyl octanoate

Gold NPs supported on CeO<sub>2</sub> were found to be an efficient catalyst for the production of octyl octanoate under base-free conditions, and reaction conditions were optimized for the ester production over this catalyst (Table 4). The utilization of toluene decreased the selectivity toward the ester (entry 1).

Entry	Conc. [mM]	T [°C]	Conv. <sup>[a]</sup> [%]	Selectivity [%] <sup>[b]</sup>		
				octanal	octanoic acid	octyl octanoate
1 <sup>[c]</sup>	2.7	100	16	31	0	69
2 <sup>[d]</sup>	2.3	100	85	1	9	63
3	0.23	100	91	1	12	70
4	0.15	80	66	2	2	82
5 <sup>[e]</sup>	0.3	80	84	1	8	79

[a] Reaction conditions: 1-octanol (0.9 mmol), H<sub>2</sub>O, Au/CeO<sub>2</sub> (Au 3 mol%), O<sub>2</sub> (0.5 MPa), 6 h. [b] Calculated on the basis of GC analysis using anisole as an internal standard. [c] 1-octanol (8 mmol), toluene (3 mL), Au 0.1 mol%, O<sub>2</sub> 0.5 MPa, 18 h. [d] Au 1 mol%, 18 h. [e] 12 h.

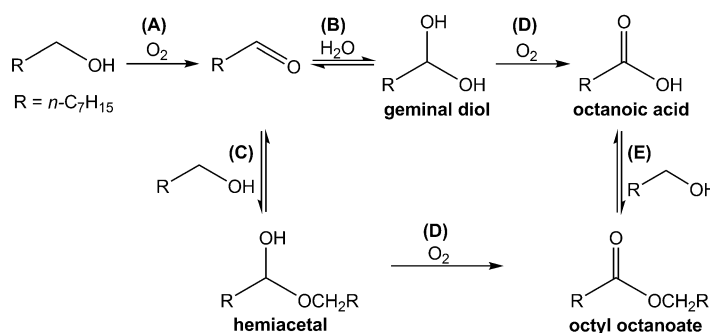
An increase in the Au loading (entry 2) along with a decrease in the concentration (entry 3) improved the reaction rate without increasing significantly the selectivity to the ester. Remarkably, a decrease in the reaction temperature (80 °C) enhanced the selectivity to ester up to 82% at moderate conversions (entry 4). The reaction conditions were further optimized and high selectivities (ca. 80%) were achieved at higher conversions (entry 5).

### Reaction pathways

Possible reaction pathways are depicted in Scheme 1. First, supported Au NPs catalyze oxidation of 1-octanol to octanal (A). There are two subsequent reaction routes: a hydration of octanal to form geminal diol (B) and an acetalization of octanal with 1-octanol to form the hemiacetal (C). The second oxidation steps (D) of geminal diol and hemiacetal yield octanoic acid

and octyl octanoate, respectively. Another route for octyl octanoate production involves esterification (E). The esterification of octanoic acid with 1-octanol was carried out by using equimolar amounts (3.9 mmol) of 1-octanol and octanoic acid in water (3 mL) over Au/NiO and Au/CeO<sub>2</sub> under the standard conditions (Au 0.1 mol%, N<sub>2</sub> 0.5 MPa, 100 °C, 6 h) (Scheme 1E). The yields of octyl octanoate were similar (i.e., 11–13%) over both catalysts. This result suggests that the difference in the product selectivity between Au/NiO and Au/CeO<sub>2</sub> can not be ascribed to the esterification efficiency. Although the reaction conditions strongly affect the product selectivity, the nature of the supports plays a pivotal role in determining the reaction pathways. Thus, Au/NiO favored route B, in contrast to Au/CeO<sub>2</sub> that promoted route C. Since both 1-octanol and octanal are immiscible in water, these compounds are probably condensed on the catalyst surface. Since the catalytic activity of Au/NiO was greatly enhanced in water as compared to other organic solvents, it is likely that Au/NiO has a high affinity to H<sub>2</sub>O, thereby forming a geminal diol. Prati and co-workers reported an increasing number of hydroxy groups on the NiO surface as a result of a decrease in the size of NiO particles.<sup>[10]</sup> This might also contribute to the high catalytic activity and the product selectivity of the Au/NiO herein prepared by CP. In contrast, 1-octanol would be relatively condensed on Au/CeO<sub>2</sub> rather than on Au/NiO. Thus, the acetalization of octanal with 1-octanol (C) was the preferred pathway over Au/CeO<sub>2</sub> surfaces.

The yields of different products under optimized conditions are represented as a function of time for Au/NiO in Figure 5. In the benzyl alcohol oxidation in water/1,4-dioxane mixture over Pt/C, benzaldehyde was the major product at conversions up to 90% above which benzoic acid was formed.<sup>[4]</sup> In contrast to these results, octanal formation was suppressed to less than 5% yield even at low conversions (< 50%) over Au/NiO. This implies that octanal is readily oxidized over Au/NiO, thereby minimizing the concentration of octanal in the reaction media and preventing the acetalization of octanal with 1-octanol. The esterification of octanoic acid with 1-octanol (Figure 5, Scheme 1E) and the hydrolysis of octyl octanoate could thus be ruled out.



**Scheme 1.** Plausible reaction pathways for the oxidation of 1-octanol over Au/NiO and Au/CeO<sub>2</sub>.



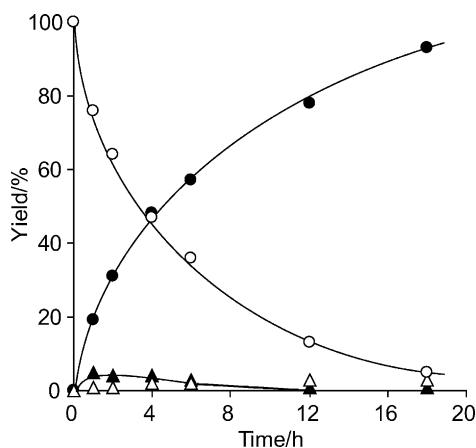


**Figure 5.** Time-yield curves for the oxidation of 1-octanol over Au/NiO. ○: 1-octanol, ▲: 1-octanol, ●: octanoic acid, △ octyl octanoate. Reaction conditions: 1-octanol (2.7 mmol), Au/NiO (Au 3 mol%), H<sub>2</sub>O (3 mL), 1,4-dioxane (9 mL), O<sub>2</sub> (0.5 MPa), 100 °C.

## Conclusions

We demonstrate the base-free oxidation of 1-octanol to octanoic acid and octyl octanoate over supported Au NPs. The product selectivity could be tuned by selecting the nature of the support. Au on NiO proved to be a highly active catalyst for the aerobic oxidation of 1-octanol to octanoic acid, with selectivities above 90%. Characterization by TEM and XAFS revealed that the conventional CP method affords small Au NPs deposited on nanometer-sized NiO particles. In contrast, Au/CeO<sub>2</sub> produces octyl octanoate directly from 1-octanol with a selectivity of 82% in a high yield. To the best of our knowledge, this is the first report on the Au-catalyzed base-free aerobic oxidation of poorly reactive aliphatic alcohols to carboxylic acids and esters as major products. Long aliphatic carboxylic acids and their alkyl esters are high-value chemicals, finding use as surfactants, lubricants, emulsifiers, and so on. These results may open the door to new green processes for producing high-value carboxylic acids and esters.

## Experimental Section

**Materials:** Tetrachloroauric acid tetrahydrate (HAuCl<sub>4</sub>·4H<sub>2</sub>O) was purchased from Tanaka Kikinzo KKK. and used as received. Reagent grades Co(NO<sub>3</sub>)<sub>2</sub>·6H<sub>2</sub>O and Ni(NO<sub>3</sub>)<sub>2</sub>·6H<sub>2</sub>O were purchased from Wako Pure Chemical. Sodium carbonate, 1-octanol, and anisole were purchased and used as received. Octyl octanoate was synthesized according to the literature.<sup>[13]</sup> High purity nanoparticulate CeO<sub>2</sub>, TiO<sub>2</sub> (P-25), and Al<sub>2</sub>O<sub>3</sub>, were supplied by Daiichi Kigenso Kagaku Kogyo, Nippon Aerosil Co., Ltd., and Mizusawa Chemicals, respectively.

**Instruments:** In order to check the presence of tiny Au clusters, high angle annular dark-field scanning transmission electron microscopy (HAADF-STEM) observations were performed by using a JEOL JEM-3000F operating at 300 kV. Specific surface area of catalysts was calculated from the nitrogen adsorption measurements. The samples were pretreated under vacuum at 200 °C for 2 h and then N<sub>2</sub> adsorption isotherms were obtained at 77 K with a SHIMADZU Tristar.

Au L<sub>3</sub>-edge X-ray absorption fine structure (XAFS) measurements were carried out at BL14B2 of SPring-8 (Hyogo, Japan).<sup>[14]</sup> The XAFS samples were ground with boron nitride in an agate mortar and made as pellets. The storage ring energy was 8 GeV with a typical current of 99.5 mA. Au L<sub>3</sub>-edge (11.9 keV) XAFS spectra of Au/NiO and Au foil were measured using a Si(311) double crystal monochromator in transmission mode. Ionization chambers were used to measure the intensity of the incident and transmitted X-rays and the Quick scan technique (QXAFS) was used in this measurement. The energy calibration was performed by taking the pre-edge peak of Cu-K edge X-ray absorption near edge structure (XANES) spectra of Cu-foil at 8980.3 eV. The spectral analysis was carried out by the XAFS analysis softwares, Athena and Artemis.<sup>[15]</sup> The extraction of the extended X-ray absorption fine structure (EXAFS) oscillation from the spectra, normalization by edge-jump, and Fourier transformation were performed by Athena. The curve-fitting analysis was carried out in *R*-space by Artemis. *k*-Range was 2–10 Å<sup>-1</sup> and *r*-range was 1.9–3.4 Å. In the curve-fitting analysis, the backscattering amplitude, the phase shift, and the mean-free path of the photoelectron were calculated by FEFF8.4, and then the other parameters, that is, the number of neighbouring atoms, the interatomic distance between the absorbed atom to the neighboring atom, the Debye–Waller factor, and the absorption edge energy were treated as fitting parameters. The intrinsic loss factor was obtained by the curve-fitting analysis of the EXAFS data of the Au-foil.

Conversions and product yields were analyzed by gas chromatography using SHIMADZU GC-14B with a Shinwa Chemical ULBON HR-1 capillary column (0.53 mm i.d., 30 m) using anisole as an internal standard. Qualitative analysis was performed with a GC–MS (SHIMADZU PARVUM2 and GC-2010 with a Shinwa Chemical ULBON HR-1 capillary column, 0.25 mm i.d., 30 m).

**Catalyst preparation:** Gold on NiO was prepared by the co-precipitation (CP) method.<sup>[11]</sup> Briefly, an aqueous solution (200 mL) containing Ni(NO<sub>3</sub>)<sub>2</sub>·6H<sub>2</sub>O (5.5 g, 19 mmol) and HAuCl<sub>4</sub>·4H<sub>2</sub>O (0.4 g, 1 mmol) was rapidly added into 0.1 M Na<sub>2</sub>CO<sub>3</sub> (240 mL) at 70 °C, and the reaction mixture was stirred at 70 °C for 1 h. The precipitate was washed with water, filtered, dried in air at 100 °C overnight, and then calcined in air at 300 °C for 4 h to obtain Au/NiO. Gold on Co<sub>3</sub>O<sub>4</sub> was prepared in a similar manner to Au/NiO but at room temperature for 3 h. Gold on CeO<sub>2</sub> was prepared by the deposition–precipitation (DP) method.<sup>[16]</sup> Gold on Al<sub>2</sub>O<sub>3</sub> was prepared by the solid grinding (SG).<sup>[17]</sup>

**Typical experiments for the aerobic oxidation of 1-octanol:** to an autoclave was charged 1-octanol (1.26 mL, 8 mmol), H<sub>2</sub>O (3 mL), Au catalyst (Au 0.1 mol%), and a magnetic stirring bar. The autoclave was purged and filled with O<sub>2</sub> until the pressure reached 0.5 MPa. The reaction mixture was stirred at 100 °C for 18 h. After the reaction, the mixture was extracted with Et<sub>2</sub>O and the organic layer was dried over Na<sub>2</sub>SO<sub>4</sub> and filtered. The filtrate was analyzed by GC–MS and GC by using anisole as an internal standard.

## Acknowledgements

This work was financially supported by JST-CREST, JST Research for Promoting Technological Seeds (A), and a Grant-in-Aid for Young Scientists (B) (21750160) from the Ministry of Education, Culture, Sports, Science, and Technology, Japan. The synchrotron radiation experiments were performed at the BL14B2 in the SPring-8 with the approval of the JASRI (2009B1007).

**Keywords:** alcohols · gold · heterogeneous catalysis · nanoparticles · oxidation

- [1] C. P. Vinod, K. Wilson, A. F. Lee, *J. Chem. Technol. Biotechnol.* **2011**, *86*, 161–171.
- [2] N. Dimitratos, J. A. Lopez-Sanchez, G. J. Hutchings, *Chem. Sci.* **2012**, *3*, 20–44.
- [3] a) G. Jenzer, M. S. Schneider, R. Wandeler, T. Mallat, A. Baiker, *J. Catal.* **2001**, *199*, 141–148; b) P. G. N. Mertens, S. L. F. Corthals, X. Ye, H.; Poelman, P. A. Jacobs, B. F. Sels, I. F. J. Vankelecom, D. E. De Vos, *J. Mol. Catal. A* **2009**, *313*, 14–21.
- [4] a) C. Donze, P. Korovchenko, P. Gallezot, M. Besson, *Appl. Catal. B* **2007**, *70*, 621–629; b) P. Korovchenko, C. Donze, P. Gallezot, M. Besson, *Catal. Today* **2007**, *121*, 13–21.
- [5] T. Wang, H. Shou, Y. Kou, H. Liu, *Green Chem.* **2009**, *11*, 562–568.
- [6] a) A. Corma, H. García, *Chem. Soc. Rev.* **2008**, *37*, 2096–2126; b) C. Della Pina, E. Falletta, L. Prati, M. Rossi, *Chem. Soc. Rev.* **2008**, *37*, 2077–2095; c) A. Abad, P. Concepcion, A. Corma, H. García, *Angew. Chem.* **2005**, *117*, 4134–4137; *Angew. Chem. Int. Ed.* **2005**, *44*, 4066–4069; d) A. Abad, A. Almela, A. Corma, H. García, *Chem. Commun.* **2006**, 3178–3180; e) A. Abad, A. Corma, H. García, *Chem. Eur. J.* **2008**, *14*, 212–222; f) P. Fristrup, L. B. Johansen, C. H. Christensen, *Chem. Commun.* **2008**, 2750–2752; g) I. S. Nielsen, E. Taarning, K. Egeblad, R. Madsen, C. H. Christensen, *Catal. Lett.* **2007**, *116*, 35–40; h) F.-Z. Su, Y.-M. Liu, L.-C. Wang, Y. Cao, H.-Y. He, K.-N. Fan, *Angew. Chem.* **2008**, *120*, 340–343; *Angew. Chem. Int. Ed.* **2008**, *47*, 334–337; i) E. Taarning, A. T. Madsen, J. M. Marchetti, K. Egeblad, C. H. Christensen, *Green Chem.* **2008**, *10*, 408–414; k) H. Liu, Y. Liu, Y. Li, Z. Tang, H. Jiang, *J. Phys. Chem. C* **2010**, *114*, 13362–13369; l) T. Ishida, M. Nagaoka, T. Akita, M. Haruta, *Chem. Eur. J.* **2008**, *14*, 8456–8460; m) T. Ishida, S. Okamoto, R. Makiyama, M. Haruta, *Appl. Catal. A* **2009**, *353*, 243–248; n) J. Yang, Y. Guan, T. Verhoeven, R. Van Santen, C. Li, E. J. M. Hensen, *Green Chem.* **2009**, *11*, 322–325; o) T. Mitsudome, A. Noujima, T. Mizugaki, K. Jitsukawa, K. Kaneda, *Adv. Synth. Catal.* **2009**, *351*, 1890–1896.
- [7] a) J. Ni, W.-J. Yu, L. He, H. Sun, Y. Cao, H.-Y. He, K.-N. Fan, *Green Chem.* **2009**, *11*, 756–759; b) A. Villa, N. Janjic, P. Spontoni, D. Wang, D. S. Su, L. Prati, *Appl. Catal. A* **2009**, *364*, 221–228.
- [8] a) C. H. Christensen, B. Jørgensen, J. Rass-Hansen, K. Egeblad, R. Madsen, S. K. Klitgaard, S. M. Hansen, M. R. Hansen, H. C. Andersen, A. Riisager, *Angew. Chem.* **2006**, *118*, 4764–4767; *Angew. Chem. Int. Ed.* **2006**, *45*, 4648–4651; b) B. Jørgensen, S. E. Christensen, M. R. D. Thomsen, C. H. Christensen, *J. Catal.* **2007**, *251*, 332–337.
- [9] a) T. Ishida, M. Haruta, *ChemSusChem* **2009**, *2*, 538–541; b) T. Takei, J. Sunenaga, K. Kuwano, H. Ohashi, T. Ishida, M. Haruta, Japanese Patent, JP2008-179978.
- [10] A. Villa, C. E. Chan-Thaw, G. M. Veith, K. L. More, D. Ferri, L. Prati, *Chem-CatChem* **2011**, *3*, 1612–1618.
- [11] M. Haruta, N. Yamada, T. Kobayashi, S. Iijima, *J. Catal.* **1989**, *115*, 301–309.
- [12] H.-G. Fritsche, R. E. Benfield, *Z. Phys. D* **1993**, *26*, 15–17.
- [13] N. Mori, H. Togo, *Tetrahedron* **2005**, *61*, 5915–5925.
- [14] a) T. Honma, H. Oji, S. Hirayama, Y. Taniguchi, H. Ofuchi, M. Takagaki, *AIP Conf. Proc.* **2010**, *1234*, 13–16; b) H. Oji, Y. Taniguchi, S. Hirayama, H. Ofuchi, M. Takagaki, T. Honma, *J. Synchrotron Radiat.* **2012**, *19*, 54–59.
- [15] B. Ravel, M. Newville, *J. Synchrotron Radiat.* **2005**, *12*, 537–541.
- [16] M. Haruta, S. Tsubota, T. Kobayashi, H. Kageyama, M. H. Genet, B. Delmon, *J. Catal.* **1993**, *144*, 175–192.
- [17] T. Ishida, N. Kinoshita, H. Okatsu, T. Akita, T. Takei, M. Haruta, *Angew. Chem.* **2008**, *120*, 9405–9408; *Angew. Chem. Int. Ed.* **2008**, *47*, 9265–9268.

Received: May 11, 2012

Revised: September 5, 2012

Published online on October 12, 2012